Stem Cell Reports, Volume 2

Supplemental Information

Programming and Isolation of Highly Pure Physiologically and Pharmacologically Functional Sinus-Nodal Bodies from Pluripotent Stem Cells

Julia Jeannine Jung, Britta Husse, Christian Rimmbach, Stefan Krebs, Juliane Stieber, Gustav Steinhoff, Andreas Dendorfer, Wolfgang-Michael Franz, and Robert David

Supplementary Material

Suppl. Table 1: Action potential parameters of cardiomyocytes derived from Tbx3 programmed cells. Related to Figure 4

Data are mean ± SD.

AP-Type	MDB (mV)	DDR (mV/s)	Overshoot (mV)	APD (ms)	Cyclelength (ms)	Plateau (ms)
Ventricular (n=9)	-50.2 ± 11.8	10.5 ± 7.5	35.8 ± 5.8	319.2 ± 134.9	896.2 ±552.5	164.5 ± 108.4
Atrial (n=3)	-53.9 ± 4.7	13.5 ± 18.2	40.6 ± 0.05	165.9 ± 66.6	650.6 ± 296.7	78.5 ± 48.0
Pacemaker system (n=15)	-47.9 ± 4.7	105.0 ± 37.6	20.5 ± 10.7	203.6 ± 96.1	342.2 ± 130.2	--
Intermediate (n=12)	-50.5 ± 6.1	52.8 ± 20.5	30.5 ± 14.6	210.4 ± 98.4	378.7 ± 123.3	66.4 ± 29.5

Suppl. Table 2: Action potential parameters of cardiomyocytes derived from control cells. Related to Figure 4

Data are mean ± SD.

AP-Type	MDB (mV)	DDR (mV/s)	Overshoot (mV)	APD (ms)	Cyclelength (ms)	Plateau (ms)
Ventricular (n=13)	-73.7 ± 4.2	3.8 ± 2.4	28.8 ± 5.5	241.1 ± 35.8	1133 ± 354.2	178.5 ± 35.3
Atrial (n=3)	-73.4 ± 7.6	4.1 ± 1.4	22.8 ± 4.0	130.7 ± 44.0	1244 ± 126.9	83.0 ± 14.5
Pacemaker system (n=6)	-57.2 ± 4.6	99.5 ± 16.5	9.8 ± 2.8	129.8 ± 19.3	567.3 ± 61.7	--
Intermediate (n=7)	-61.1 ± 7.4	48.2 ± 5.7	23.5 ± 9.0	203.3 ± 58.9	566.4 ± 248.7	59.7 ± 25.1

Suppl. Table 3: Action potential parameters of cardiomyocytes derived from iSABs. Related to Figure 4

Data are mean ± SD.

AP-Type	MDB (mV)	DDR (mV/s)	Overshoot (mV)	APD (ms)	Cyclelength (ms)	Plateau (ms)
Mat. Pacemaker system (n=43)	-54.7 ± 3.7	116.7 ± 85.3	21.6 ± 7.6	86.2 ± 28.2	197.4 ± 63.2	--
Early Pacemaker system (n=10)	-60.4 ± 3.5	108.8 ± 102.0	28.7 ± 24.1	114.5 ± 97.4	263.3 ± 154.7	33.7 ± 32.6

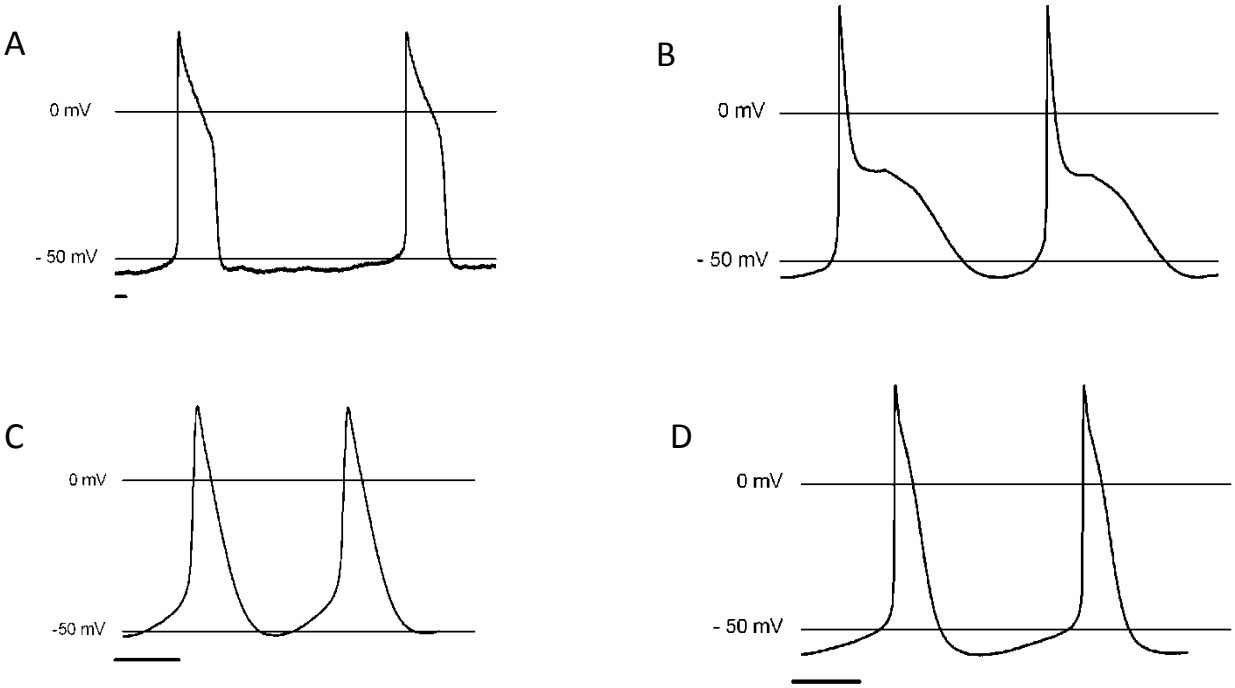
A
0 mV
- 50 mV
B
0 mV
- 50 mV
C
0 mV
-50 mV
D
0 mV
- 50 mV

Suppl. Fig. 1: Representative Action Potentials derived from Tbx3 programmed cells. Related to Figure 4

(A, B) Myocardial types with (A) ventricular-like and (B) atrial-like action potentials. (C, D) Pacemaker type action potentials, with (C) mature sinoatrial-like action potentials and (D) slightly immature pacemaker-like cells referred to as intermediate type cells of the murine embryonic heart. Horizontal time bar: 100 ms.

A

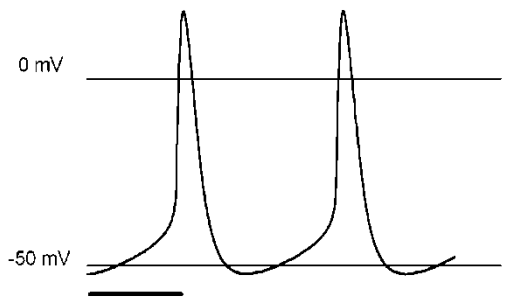

B

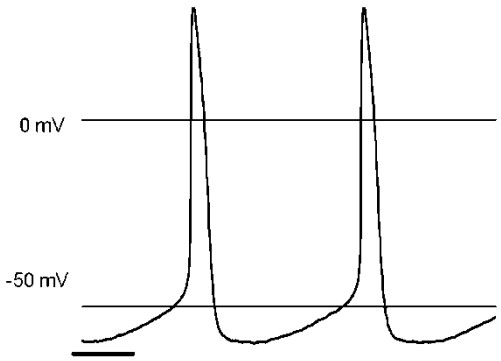

Suppl. Fig. 2: Representative Action Potentials derived from iSAB-cardiomyocytes. Related to Figure 4

(A) Pacemaker type action potentials resembling action potentials generated by adult murine sinoatrial node cells. (B) action potentials generated by slightly immature pacemaker-like cells. Horizontal time bar: 100 ms.

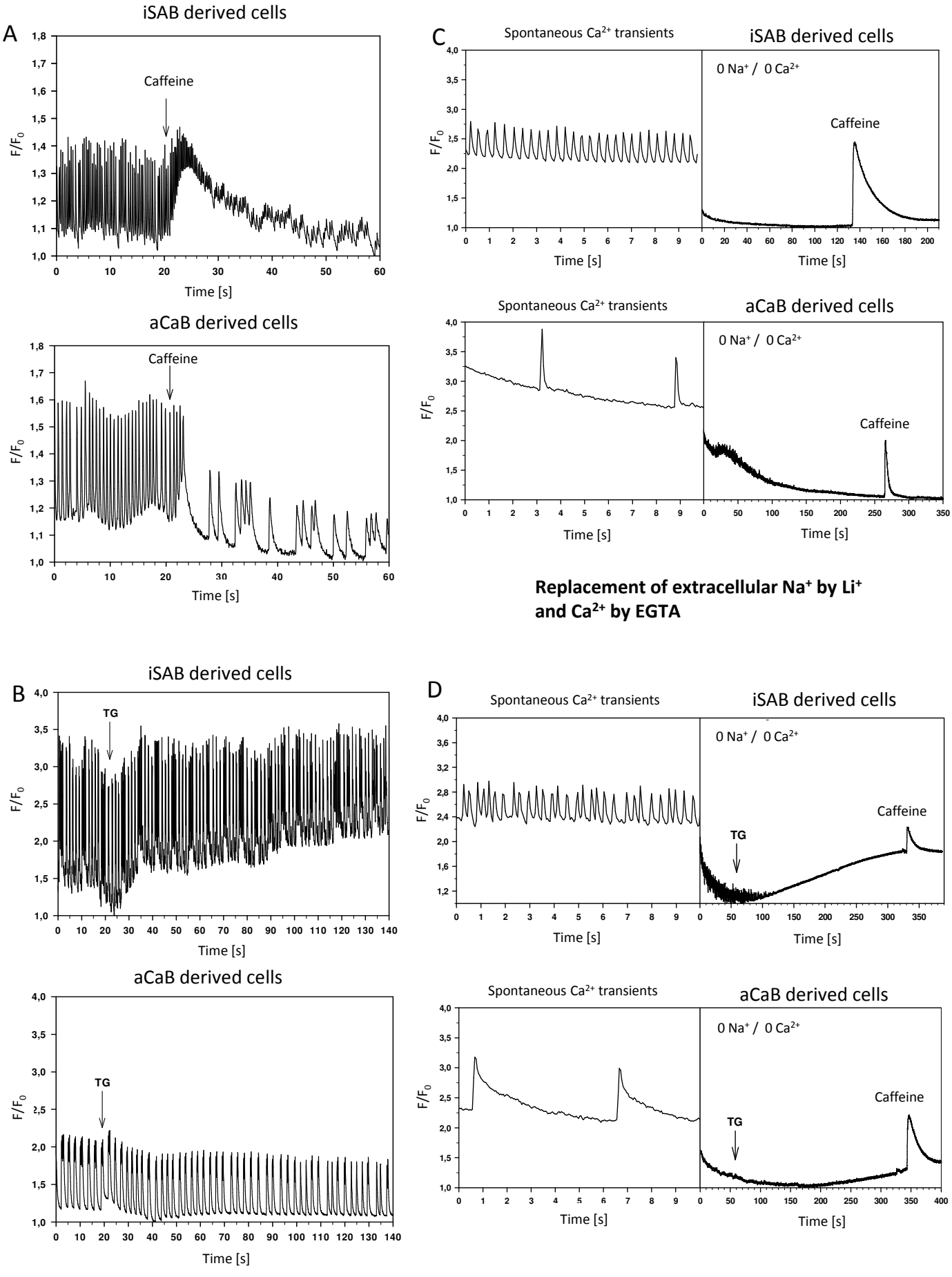
A
iSAB derived cells
Caffeine
F/F0
Time [s]
aCaB derived cells
Caffeine
F/F0
Time [s]
C
Spontaneous Ca2+ transients
iSAB derived cells
0 Na+ / 0 Ca2+
Caffeine
F/F0
Time [s]
Time [s]
Spontaneous Ca2+ transients
aCaB derived cells
0 Na+ / 0 Ca2+
Caffeine
F/F0
Time [s]
Time [s]
Replacement of extracellular Na+ by Li+
and Ca2+ by EGTA
B
iSAB derived cells
TG
F/F0
Time [s]
aCaB derived cells
TG
F/F0
Time [s]
D
Spontaneous Ca2+ transients
iSAB derived cells
0 Na+ / 0 Ca2+
Caffeine
TG
F/F0
Time [s]
Time [s]
Spontaneous Ca2+ transients
aCaB derived cells
0 Na+ / 0 Ca2+
Caffeine
TG
F/F0
Time [s]
Time [s]

Suppl. Fig. 3: Calcium Characterisitics of pacemaker-like cardiomyocytes obtained from iSABs. Related to Figure 5

(A) Spontaneaous Ca^{2+}-transients before and in the presence of 10 mM Caffeine in iSAB and aCaB derived cells. The amplitude of the Caffeine-induced peak in the former is comparable to the maxima of spontaneous Ca^{2+}-transients. n≥8 (B) Blockage of Ca^{2+} uptake into the SR via Thapsigargin leads to increased diastolic Ca^{2+} levels in iSAB derived as opposed to aCaB derived cells. n≥11. (C) Ca^{2+}-transients before and after blockage of the Na^{+}/ Ca^{2+} exchanger and sarcolemmal Ca^{2+} channels: a large caffeine peak is observed in iSAB derived cells as opposed to aCaB derived cells. n>16. (D) Ca^{2+} transients before and after inhibition of Ca^{2+} uptake: Na^{+}/ Ca^{2+} exchanger inhibition plus SERCA inhibition causes a rapid increase of intracellular Ca^{2+} in iSAB derived cells as opposed to aCaB derived cells. n>24. In addition, a small Caffeine peak appears in each case.

Suppl. Movie 1 Related to Figure 3
Increased and more vigorous spontaneous beating activity in EBs derived from TBX3 programmed cells combined with *Myh6*-promoter based antibiotic selection; Beating rate: 194 beats per min.

Suppl. Movie 2 Related to Figure 3
Controls related to Suppl Movie 3: unprogrammed cells after Myh6-promoter based antibiotic selection; Beating rate: 86 beats per min.

Suppl. Movie 3 Related to Figure 3
Typical induced sinoatrial bodies (iSABs) after additional decollating.

Suppl. Movie 4 Related to Figure 3
Highly synchronized cell layer beating at >350 beats per minute after further cultivation of iSABs on gelatine coated dishes for three weeks. Synchronisation was analysed via Keyence VW9000 Motion Analyser software.

Suppl Movie 5 Related to Figure 3
Typical beating spindle and spider cells derived from iSABs.

Suppl. Movie 6 Related to Figure 5
Calcium transients recorded from a typical iSAB.

Suppl. Movie 7 Related to Figure 6
Pacing of host slice tissue via an iSAB. The identical iSAB is shown in Fig. 6E demonstrating transmission of Calcein dye over time. ~30 beats per min are achieved in the host slice as compared to a maximum of ~60 beats per min via electrode stimulation.

Suppl. Movie 8 Related to Figure 6
iSAB based stimulation of adjacent slice regions leads to synchronized Ca^{2+} transients as evident from Fluo-4/AM imaging. Please refer to Fig. 6F and 6G, showing the identical iSAB, for detailed analysis.